Pseudo 2D elastic waveform inversion for Q factor in the near surface

Yue Wang, Jie Zhang, University of Science and Technology of China (USTC)*

Summary

Seismic wave propagation is significantly affected due to the complexity in the near surface area. Therefore, it is important for subsurface imaging to obtain the near surface information as much as possible. Seismic attenuation, described by the quality or Q factor, has great effect on the seismic waveform. But it is rarely estimated for the near surface area. We develop a pseudo 2D elastic waveform inversion for determining Q_P factor in the shallow near surface area. The input data are the early arrival waveforms in the CMP domain. For the forward elastic wavefield modeling, we use a discrete wavenumber method for 1-D layer models. For inverting a Q_P model with fixed velocity structures, we apply a conjugate gradient method to solve a 2D problem. The output Q_P model is in 2D. We test our method on synthetics and also apply this method to field data from an oil field in China.

Introduction

As seismic wave travels through the earth, its energy is converted into heat due to anelasticity and heterogeneity of the earth. The loss of energy means attenuation and dispersion (Futterman, 1962). It is very important to determine a reliable Q structure for accurate full waveform simulation. By now, Q factor is routinely estimated and applied for imaging for deep structures (Bennington *et al*., 2008), but it is usually ignored in the near surface area. Once we get the reliable Q structure of this area, then we can perform waveform inversion using true amplitudes to solve other typical problems such as velocity structure inversion. Currently, full waveform inversion techniques focus on fitting normalized amplitude in an L_2 norm of the objective function (Sambridge *et al*., 1991) or maximizing a cross-correlation objective function that indirectly utilize amplitude information (Luo and Schuster, 1991).

In this study, we apply seismic early arrival waveform inversion in the time domain to estimate two dimensional structure of Q factor in the near surface area. The input data is sorted into CMP domain. In general, 1D forward modeling is applied to do 1D model inversion, while 2D forward modeling is applied for 2D model inversion. However, such 2D inversion is much more time consuming than 1D inversion (Zhou et al., 1993, 1995; Pratt and Shipp, 1999). We develop a method that applies 1D forward modeling to invert for a 2D structure model. However, using 1D forward modeling to invert for a 2D structure is not accurate. This method can only deal with approximate 1D structure which may have small anomalies.

Method

For forward modeling, we use a discrete wavenumber method (Bouchon and Aki, 1977). The elastic velocity can be expressed as (Aki and Richards, 1980):

$$\mathrm{v}(\omega) = \mathrm{v}_1[1 + \frac{1}{\pi Q}\ln\left(\frac{\omega}{2\pi}\right) - \frac{i}{2Q}]. \quad (1)$$

Here, v_1 represents the velocity of elastic waves at frequency 1 Hz and v (ω) represents the velocity of elastic wave at frequency ω. Q is the attenuation factor for elastic waves. We can consider that Q is not variable with frequency for the frequency band that ranges from 0.2 Hz to 100 Hz. Seismic forward modeling can simply be expressed:

$$\mathbf{d} = \mathbf{G}(\mathbf{m}), \quad (2)$$

where **d** is the seismic data vector, ***m*** is the parameter vector (e.g., Q_P model), and **G** is the operator matrix. In this study,

$$\boldsymbol{m} = (Q_1, Q_2, \ldots, Q_k)^T, \quad (3)$$

where *k* is the number of Q_P layers in the near surface area. We apply a conjugate gradient method to solve the inversion problem of equation (2) (Hestenes and Stiefel, 1952; Fletcher and Reeves, 1964). The norm of the objective function is

$$\boldsymbol{\varphi}(\mathbf{m}) = \frac{1}{2}\sum_{j=1}^{n}\left\|d_{obs}^{j} - d_{syn}^{j}\right\|^2 + \frac{1}{2}\tau\|\mathbf{Rm}\|^2. \quad (4)$$

We use a two-term forward finite-difference operator (Equation 5) to compute the partial derivatives of data with respect to Q_P:

$$\frac{\partial \mathbf{d}(m_i,t)}{\partial m_i} = \frac{\mathbf{d}(m_i+\Delta m_i,t) - \mathbf{d}(m_i,t)}{\Delta m_i}, \quad (5)$$

where **d** (m_i, t) is the seismic data record at time *t*, m_i is the *i*th model parameter and Δm_i is a small perturbation in the *i*th model parameter.

Figure 1 shows how to use a 1D forward model to invert for 2D. If the thickness of each layer is thin enough, we can assume the structure to be layered models locally. So we can use $\mathbf{d_1}$ to invert for m_1, m_2, m_3 and m_4; $\mathbf{d_2}$ to invert for m_5, m_6, m_7 and m_8; $\mathbf{d_3}$ to invert for m_9, m_{10}, m_{11}, m_{12}; $\mathbf{d_4}$ to invert for m_{13}, m_{14}, m_{15}, m_{16}; $\mathbf{d_5}$ to invert for m_{17}, m_{18}, m_{19}, m_{20}, and so on. Using a conjugate gradient method, we can invert for all parameters simultaneously. In other words, all values of **m** parameter are inverted locally but they form a pseudo 2D model to output.

DOI http://dx.doi.org/10.1190/segam2014-1053.1

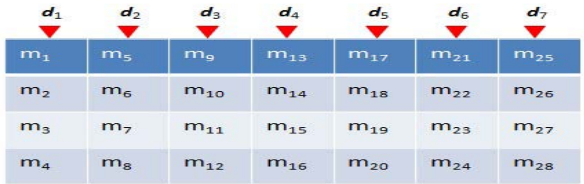

Figure 1: A 2D model structure. From m_1 to m_{28} are model parameters to be inverted. From d_1 to d_7 are data measured on the surface. Red triangles are receivers on the surface.

Synthetic test

To test this method, we design a simple three-layer model with different Q_P and P-wave velocity in each layer, and V_P/V_S is assumed 3.0 to make sure the early arrivals have little S waves information. The model parameters are listed in Table 1 and the Q_P structure is shown in Figure 2(a). In Figure 2(a), there are two anomalies from a 1D stratified medium, an elevated and a depressed interface. It can be dealt with as a locally layered medium. So we set a seven-layer structure as an initial model, listed in Table 2, and the Q_P structure is shown in Figure 2(b). Table 2 lists P-wave velocities, S-wave velocities, Q_S, the thickness and the density of each layer. The early arrivals are mostly associated with direct P, P-wave refraction, P-wave reverberations, and wide-angle P reflections. Thus, we can use early arrivals to invert for Q_P (Wang and Zhang, 2013).

layer	V_P (m/s)	V_S (m/s)	thickness (m)	density (g/cm^3)	Q_S
1	1700	566.7	150.0	1.800	15.00
2	2100	700.0	150.0	2.000	25.00
3	2400	800.0	∞	2.200	40.00

Table 1: The true model parameters include P-wave velocity, S-wave velocity, Q_S value, thickness and density of each layer.

layer	V_P (m/s)	V_S (m/s)	thickness (m)	density (g/cm^3)	Q_S
1	1700	566.7	50.0	1.800	15.00
2	1700	566.7	50.0	1.800	15.00
3	1700	566.7	50.0	1.800	15.00
4	2100	700.0	50.0	2.000	25.00
5	2100	700.0	50.0	2.000	25.00
6	2100	700.0	50.0	2.000	25.00
7	2400	800.0	∞	2.200	40.00

Table 2: Initial model parameters include P-wave velocity, S-wave velocity, Q_S value, thickness and density of each layer.

After 10 iterations, we obtain the inverted Q_P structure shown in Figure 2(c). The shallow blue part can be inverted well. The high Q_P and low Q_P areas are retrieved in this inversion result. We select four traces to compare the waveforms as shown in Figure 3. The waveforms are fitted well after10 iterations. The data misfit over iterations is shown in Figure 4. It descends quickly and this method has converged.

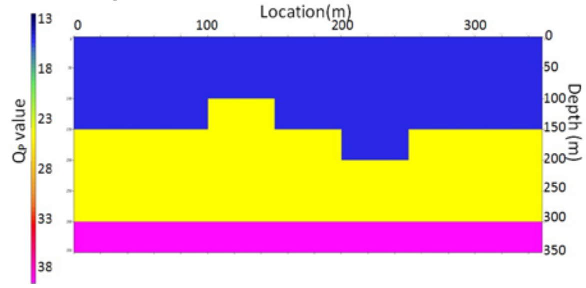

(a)

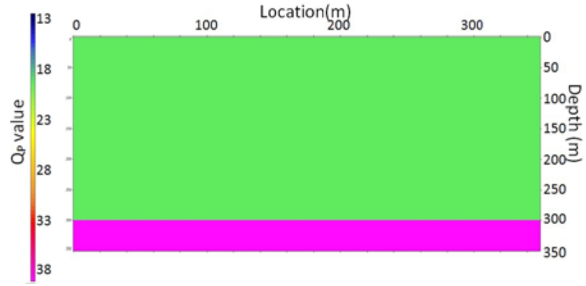

(b)

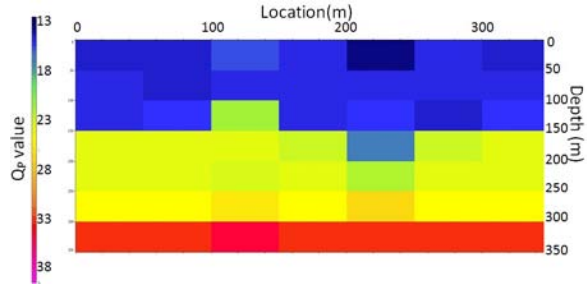

(c)

Figure 2: (a) The true Q_P structure for inversion. (b) Initial Q_P model for input. (c) Inversion result of Q_P model after 10 iterations.

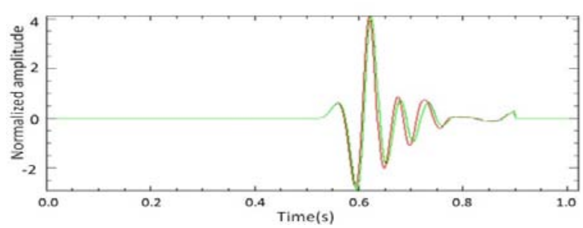

(a)

DOI http://dx.doi.org/10.1190/segam2014-1053.1

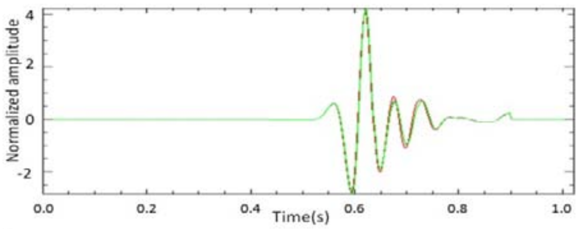

(b)

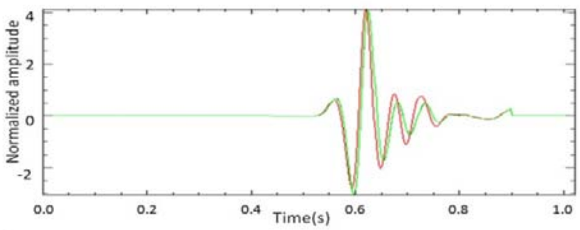

(c)

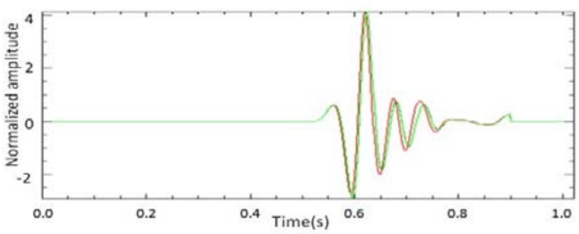

(d)

Figure 3: Waveform comparison of the inversion. Black line is for true model, red line is for initial model and green line is for inversion result after 10 iterations. (a) Waveforms of the first trace. (b) Waveforms of the third trace. (c) Waveforms of the fifth trace. (d) Waveforms of the seventh trace.

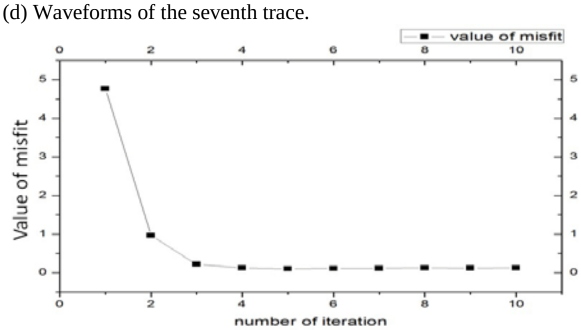

Figure 4: Inversion data misfit of waveforms versus iteration number.

Field data test

We apply the pseudo 2D waveform inversion method to field data from an oil field in China. We select twenty traces from the dataset, covering 600 m long. The offset of all the selected traces is 500 meters. The source depth of shots is 6 m. The time window of each trace is 1.0 s. We mute noise before the first arrivals. We apply a band-pass filter to the field data and keep the frequency range from 2 Hz to 20 Hz. Figure 5 shows the selected 20 traces from the field data. Table 3 shows the initial 1D model parameters, including the P-wave velocity, the S-wave velocity, Q_S value, the thickness, and the density of each layer. The initial Q_P model is shown in Figure 6(a). The inverted Q_P model after 10 iterations is shown in Figure 6(b). Figure 7 shows a comparison of waveforms for the field data, the initial model and the inverted model. One reason for the waveforms cannot be fitted exactly is that the velocity structure of this area is not accurate. We compare the norm of the data misfit in Figure 8: the conjugate gradient scheme converged. The inverted model shows that the Q_P values are very low in near surface and it contains two relative high Q_P anomalies in this area. Based on the near offset, the structure of shallow 150 meters or even 200 meters is more reliable than deeper structure.

layer	V_P (m/s)	V_S (m/s)	thickness (m)	density (g/cm^3)	Q_S
1	1557	519	30.0	1.80	10.00
2	1700	671	30.0	2.00	20.00
3	2087	672	30.0	2.00	20.00
4	2127	676	30.0	2.00	20.00
5	2184	678	30.0	2.00	20.00
6	2215	727	30.0	2.20	20.00
7	2240	767	30.0	2.20	20.00
8	2290	769	30.0	2.20	20.00
9	2310	773	30.0	2.20	20.00
10	2350	800	∞	2.30	50.00

Table 3: An initial model for field data inversion includes P-wave velocity, S-wave velocity, Q_S value, thickness and density of each layer.

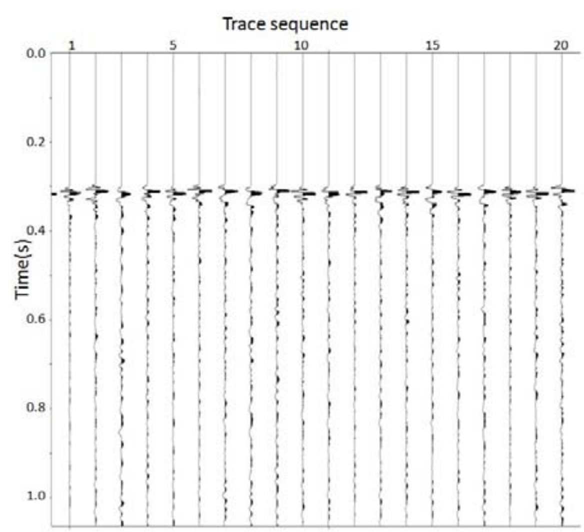

Figure 5: Selected 20 traces from an oil field.

DOI http://dx.doi.org/10.1190/segam2014-1053.1

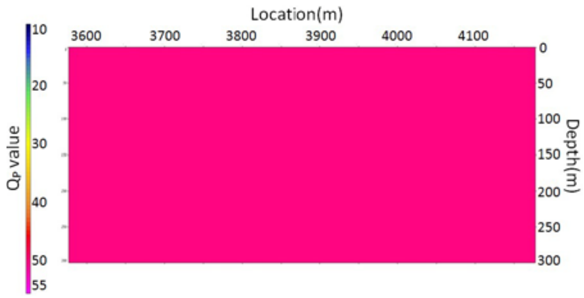

(a)

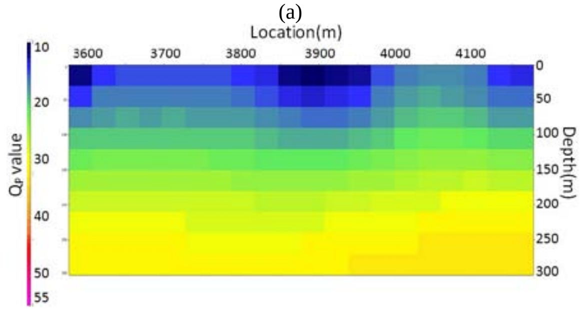

(b)

Figure 6: (a) The initial Q_P structure. (b) Inversion result of Q_P model after 10 iterations.

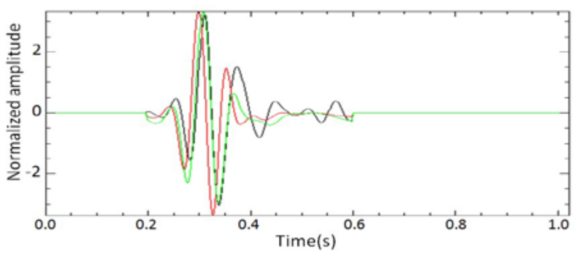

(a)

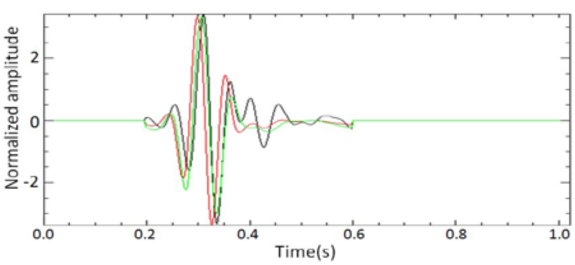

(b)

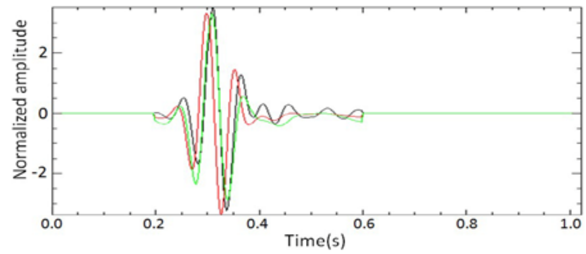

(c)

Figure 7: Waveform comparison. Black line represents true data, red line is for initial model and green line is for inversion result after 10 iterations. (a) The 4th traces comparison. (b) The 17th traces comparison. (c) The 20th traces comparison.

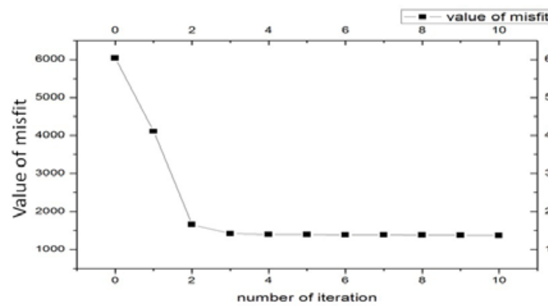

Figure 8: Inversion data misfit versus iteration number.

Conclusions

We developed a pseudo 2D elastic waveform inversion for Q factor in the near surface. This method is computationally much faster than a full 2D elastic method. Numerical tests confirm that pseudo 2D elastic waveform inversion for Q factor in the near surface is reliable if the structure in the near surface can be dealt as layered model with small fluctuation. If the structure is complex, this method does not work. We applied this method to field data from an oil field in China. The results show us this area has strong attenuation in the near surface and there are two relative high Q_P anomalies. Low Q_P values have great influence on seismograms so our inversion method can help image useful information about the approximately layered near surface.

Acknowledgments

We appreciate Prof. Michel Bouchon for offering an elastic forward modeling program. We also thank our research group for helpful advice during this project.

DOI http://dx.doi.org/10.1190/segam2014-1053.1

http://dx.doi.org/10.1190/segam2014-1053.1

EDITED REFERENCES

Note: This reference list is a copy-edited version of the reference list submitted by the author. Reference lists for the 2014 SEG Technical Program Expanded Abstracts have been copy edited so that references provided with the online metadata for each paper will achieve a high degree of linking to cited sources that appear on the Web.

REFERENCES

Aki, K., and P. G. Richards, 1980, Quantitative seismology: Theory and methods: W. H. Freeman and Company.

Bennington, N., C. Thurder, and S. Roecker, 2008, Three-dimensional seismic attenuation structure around the SAFOD Site, Parkfield, California : Bulletin of the Seismological Society of America, **98**, no. 6, 2934–2947, http://dx.doi.org/10.1785/0120080175.

Bouchon, M., and K. Aki, 1977, Discrete wave-number representation of seismic-source wave fields: Bulletin of the Seismological Society of America, **67**, 259–277.

Fletcher, R., and C. M. Reeves, 1964, Function minimization by conjugate gradients: The Computer Journal, **7**, no. 2, 149–154, http://dx.doi.org/10.1093/comjnl/7.2.149.

Futterman, W. I., 1962, Dispersive body waves: Journal of Geophysical Research, **67**, no. 13, 5279–5291, http://dx.doi.org/10.1029/JZ067i013p05279.

Hestenes, M. R., and E. Stiefel, 1952, Methods of conjugate gradients for solving linear systems: Journal of Research NBS, **49**, 409–436.

Luo, Y., and G. T. Schuster, 1991, Wave-equation traveltime inversion: Geophysics, **56**, 645–653, http://dx.doi.org/10.1190/1.1443081.

Pratt, R. G., and R. M. Shipp, 1999, Seismic waveform inversion in the frequency domain, Part 2: Fault delineation in sediments using crosshole data: Geophysics, **64**, 902–914, http://dx.doi.org/10.1190/1.1444598.

Sambridge, M. S., A. Tarantola, and B. L. N. Kennett, 1991, An alternative strategy for nonlinear inversion of seismic waveforms: Geophysical Prospecting, **39**, no. 6, 723–736, http://dx.doi.org/10.1111/j.1365-2478.1991.tb00341.x.

Wang, Y., and Jie Zhang, 2013, Elastic early-arrival waveform inversion for Q-factor in the near surface: 83rd Annual International Meeting, SEG, Expanded Abstracts, doi: 10.1190/segam2013-0963.1.

Zhou, C., W. Cai, Y. Luo, G. Schuster, and S. Hassanzadeh, 1993, High-resolution cross-well imaging by seismic traveltime + waveform inversion: The Leading Edge, **12**, 988–993, http://dx.doi.org/10.1190/1.1436918.

Zhou, C., W. Cai, Y. Luo, G. T. Schuster, and S. Hassanzadeh, 1995, Acoustic wave-equation traveltime and waveform inversion of crosshole seismic data: Geophysics, **60**, 765–773, http://dx.doi.org/10.1190/1.1443815.